RESEARCH ARTICLE

ADVANCED MATERIALS INTERFACES
www.advmatinterfaces.de

Thickness-Dependent Energy-Level Alignment at the Organic–Organic Interface Induced by Templated Gap States

*Jan Hagenlocher, Katharina Broch, Matthias Zwadlo, Daniel Lepple, Jonathan Rawle, Francesco Carla, Satoshi Kera, Frank Schreiber, and Alexander Hinderhofer**

Planar organic heterostructures are widely explored and employed in photovoltaic cells, light-emitting diodes, and bilayer field-effect transistors. An important role for device performance plays the energy level alignment at the inorganic–organic and organic–organic interfaces. In this work, incremental ultraviolet photoelectron spectroscopy measurements and real-time X-ray scattering experiments are used to thoroughly investigate the thickness-dependent electronic and structural properties of a perfluoropentacene (PFP)-on-[6]phenacene heterostructure. For both materials an incremental increase of the material work function (positive interface dipole) is found. For [6]phenacene, this can be assigned to a thickness-dependent change of molecular arrangement evident from a change of the unit cell volume and a consequential alteration of the ionization energy. In the case of PFP the interface dipole stems from charge transfer from the substrate into unoccupied molecular orbitals resulting in an electrostatic potential on the surface. The magnitude of this potential can be correlated with an increased gap state density resulting from templated structural defects mediated by the bottom layer.

1. Introduction

The energy level alignment (ELA) at organic/organic interfaces is a key aspect affecting the performance of various organic optoelectronic devices.[1] For example, in organic solar cells, the energy offset between the donor material's highest occupied molecular orbital (HOMO) level and the lowest unoccupied molecular orbital (LUMO) level of the acceptor material determines the value of the open circuit voltage.[2] Despite its relevance for device functionality and considerable research efforts, a unifying mechanism to predict the ELA remains controversial and the reactivity of the substrate material employed has to be considered.[3] An ELA mechanism valid for inert surfaces takes into account the density of gap states caused by structural imperfections in the molecular packing.[4] The gap state region starts from the respective HOMO and LUMO edges and gradually decreases into the energy gap with an exponential tail. By controlling the density of structural imperfections, it is possible to control the density of gap states and their extension into the gap.[5] This was demonstrated by exposure of organic materials to different gases, which was reported to affect the ELA and charge transport properties by diffusion of gas molecules into the organic films and consequential changes in the molecular packing.[6] Another approach is to use different substrate temperatures during the growth of organic heterostructures, which can significantly influence the structural and morphological properties of not only the bottom layer but also the layer grown on top.[7] The bottom layer thereby acts as a template affecting the orientation and crystalline quality of the top layer.[8]

In this work, we report the thickness-dependent impact of different substrate temperatures on the structural and electronic properties of a planar [6]phenacene/perfluoropentacene ([6]phen/PFP) heterostructure on silicon oxide (SiO_2), investigated by in situ X-ray reflectivity (XRR) and grazing incidence X-ray diffraction (GIXD) as well as ultralow background, high-sensitivity ultraviolet photoelectron spectroscopy (UPS). [6]phenacene, consisting of six benzene rings fused together in a zigzag fashion, has caught extended interest due to its high stability against ambient conditions and its remarkably high field effect mobilities.[9] PFP is known for its high ionization potential as well as its high electron mobility and is often used as an acceptor material in organic heterojunctions.[10] Both

J. Hagenlocher, K. Broch, M. Zwadlo, D. Lepple, F. Schreiber, A. Hinderhofer
Institute for Applied Physics
University of Tübingen
72726 Tübingen, Germany
E-mail: alexander.hinderhofer@uni-tuebingen.de
J. Rawle, F. Carla
Diamond Light Source
Didcot, Oxon OX11 0DE, UK
S. Kera
Department of Photo-Molecular Science
Institute for Molecular Science
Okazaki 444-8585, Japan
The ORCID identification number(s) for the author(s) of this article can be found under https://doi.org/10.1002/admi.202101382.

DOI: 10.1002/admi.202101382

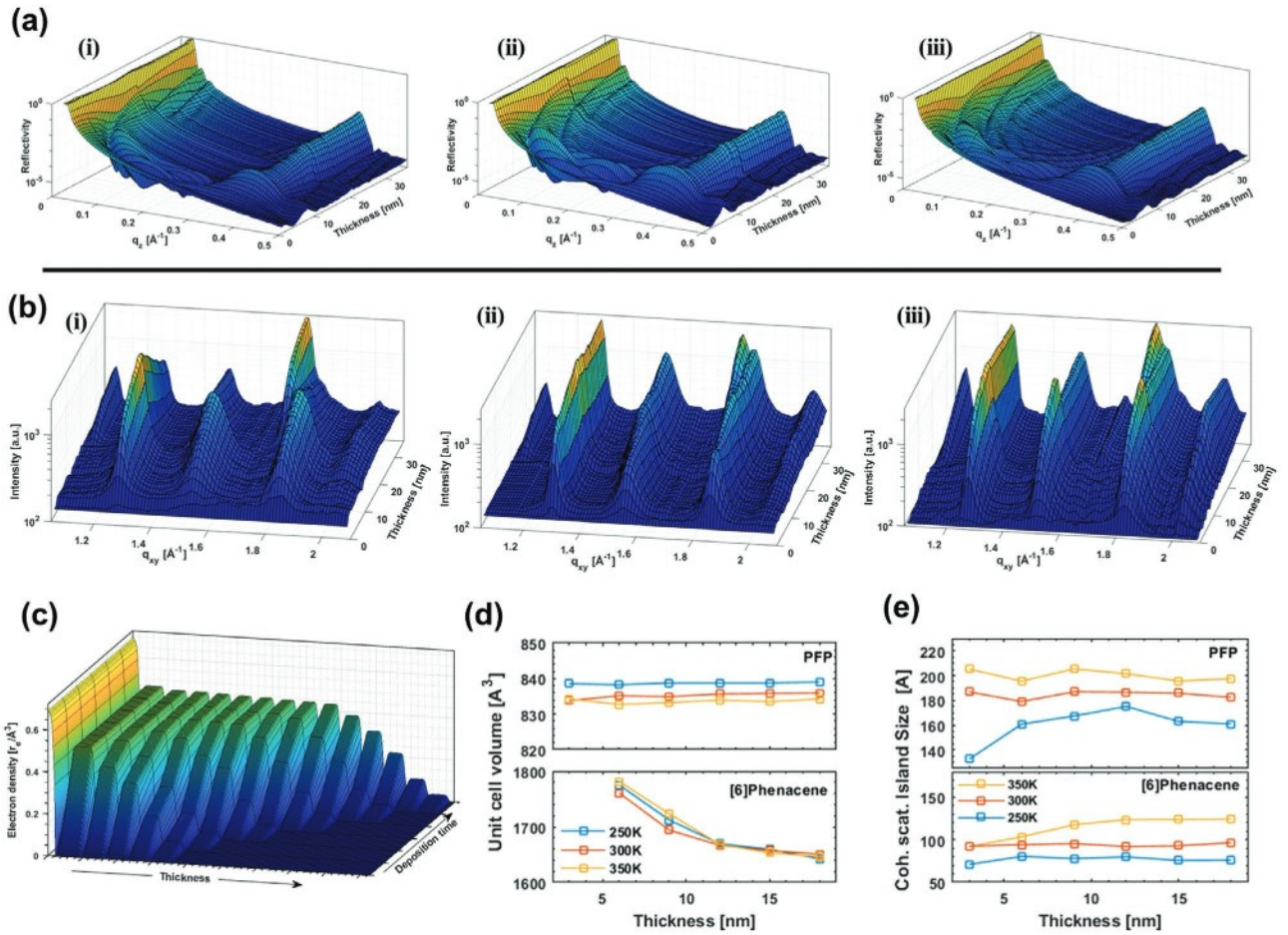

Figure 1. a) In situ XRR data of the heterostructures (i) [6]phenacene grown at 250 K substrate temperature, (ii) at 300K and (iii) at 350K. b) In situ GIXD data of the same heterostructure. c) Electron density of [6]phenacene grown at room temperature. d) Thickness dependent unit cell volume of the [6]phenacene (bottom) and PFP (top) films. e) In-plane coherently scattering island size of the [6]phenacene and PFP thin films obtained from Scherrer's formula.

materials were grown to a thickness of 18 nm using organic molecular beam deposition.[11]

2. Results and Discussion

2.1. Structural Characterization

First, we discuss the structure of the different heterostructures, since this information is vital for the evaluation of the electronic properties in the next section. **Figure 1**a shows the real-time XRR data of the heterostructures where the bottom [6]phenacene (thickness 0 to 18 nm) layer was grown at a substrate temperature of T = i) 250, ii) 300, and iii) 350 K. After the growth of [6]phenacene was finished the system was given time to equilibrate to room temperature before the growth of the top PFP layer (thickness 18–36 nm) was started, so that all PFP films were deposited at the same substrate temperature on the [6]phenacene layer.

Evident from the more pronounced Kiessig oscillations ($q_z \approx 0.05$–0.15 Å^{-1}) in (ii) and (iii) we can conclude that increasing the substrate temperature leads to overall smoother [6]phenacene films. Interestingly, with deposition of PFP on top of the low temperature sample Kiessig oscillations appear, meaning the overall roughness is decreasing and, after 18 nm, does not differ compared to the higher temperatures (see also Figure S1, Supporting Information). This behavior can be explained with PFP molecules diffusing down the [6]phenacene terraces where they accumulate and fill the space between grains.[12]

Another feature are Laue fringes originating from the coherently scattering crystal size along the z-direction surrounding the Bragg reflection. Their appearance correlates with the length scale of crystalline coherence and indicates larger coherently scattering domains for higher temperatures.

Analyzing the Bragg peak position for the different thicknesses, we find a shift toward higher q_z- values with higher film thickness for the bottom [6]phenacene layer. Converted into a real-space value, this is equivalent to the lattice spacing decreasing, meaning the molecular tilt angle Θ relative to the substrate is changing. A schematic representation can be found in Supporting Information. This appears to be a generally thickness-dependent effect which was further investigated by an electron density fit for the sample grown at room temperature

Table 1. Unit cell parameters and unit cell volume V_{UC} of the 18 nm [6]phenacene and PFP films, respectively.

	[6phenacene				PFP			
	a [Å]	*b* [Å]	*c* [Å]	V_{UC} [Å^3]	*a* [Å]	*b* [Å]	*c* [Å]	V_{UC} [Å^3]
250 K	8.2(3)	6.2(2)	32.0(0)	1638.0(1)	4.5(5)	11.5(5)	15.9(8)	839.0(2)
300 K	8.3(8)	6.2(1)	31.6(8)	1648.6(2)	4.5(3)	11.5(5)	15.9(8)	835.9(4)
350 K	8.3(9)	6.2(4)	31.4(8)	1648.0(1)	4.5(3)	11.5(5)	15.9(5)	834.2(5)

(Figure 1c and Supporting Information). We find the lattice spacing of the two first layers to be significantly larger (18.7 and 16.7 Å) than for the subsequent layers, for which the spacing stays constant. The same behavior is found also for the samples grown at higher and lower temperature, however, the final out-of-plane lattice spacing is different (see **Table 1**). Since PFP also grows in a standing up configuration and due to its almost identical long axis length compared to [6]phenacene molecules, the observed Bragg peak does not visibly deviate with the start of PFP deposition, but rather stays at a constant q_z position corresponding to a lattice spacing of ≈15.8 Å and implying that the top layer PFP out-of-plane structure is not thickness dependent.

Figure 1b shows GIXD data of [6]phen/PFP heterostructures. All three heterostructures exhibit several in-plane Bragg reflections corresponding to nearly standing molecules and the short axis (ab-plane) of the unit cell parallel to the substrate plane. For [6]phenacene, the Bragg reflection positions after deposition of 18 nm are moderately temperature dependent, leading to the unit cell parameters summarized in Table 1 and showing good agreement with a recently published crystal structure.[13] Figure 1d (bottom) shows the thickness dependence of V_{UC} taking also the out-of-plane data into account. We find an overall decrease of V_{UC} between 6 and 12 nm and a weak decrease between 12 and 18 nm. V_{UC}, shown in Table 1, differs only slightly between the different substrate temperatures for the films at the final thickness of 18 nm.

From the peak width of the in-plane reflections, the in-plane coherently scattering island size (D_{coh}) of the three films is estimated. For T = 350 K, D_{coh} is increasing from 91.2 to 124.5 Å between 3 and 18 nm. The 300 and 250 K samples show only a negligible thickness dependence but depend on the temperature with D_{coh} being 96.5 (300 K) and 75.9 Å (250 K) (Figure 1e, bottom). Since D_{coh} depends on defects and strain which reduce the long-range crystalline order in the thin films, we can conclude that increasing the temperature leads to higher crystallinity. Interestingly, also PFP exhibits an increased crystallinity when the [6]phenacene layer beneath was grown at high temperature, an templating effect also found in PFP grown on diindenoperylene layers.[8a] We find D_{coh} for PFP to be 160.9, 182.3, and 197.5 Å for the 250, 300, and 350 K sample, respectively (Figure 1e, top). The Bragg reflection position is not affected by the bottom layer and thickness, as evident from Figure 1d, top), where the unit cell volume is plotted versus the thickness (see also Table 1).

2.2. UPS Data [6]Phenacene

In order to obtain a thorough understanding of the electronic properties of the entire heterostructure we next discuss the ELA of [6]phenacene on the SiO_2-substrate. **Figure 2** shows the UPS data for the different substrate temperatures during growth dependent on film thickness.

On the respective left-hand side, the HOMO region is plotted, on the right-hand sight the corresponding secondary electron cut-off (SECO). Interestingly, the overall HOMO shape and the binding energy E_{Bind} (as determined from the HOMO onset and indicated by short vertical lines) is affected neither by the substrate temperature nor by the film thickness, with an average value of 1.51 ± 0.02 eV (see **Figure 3**, bottom).

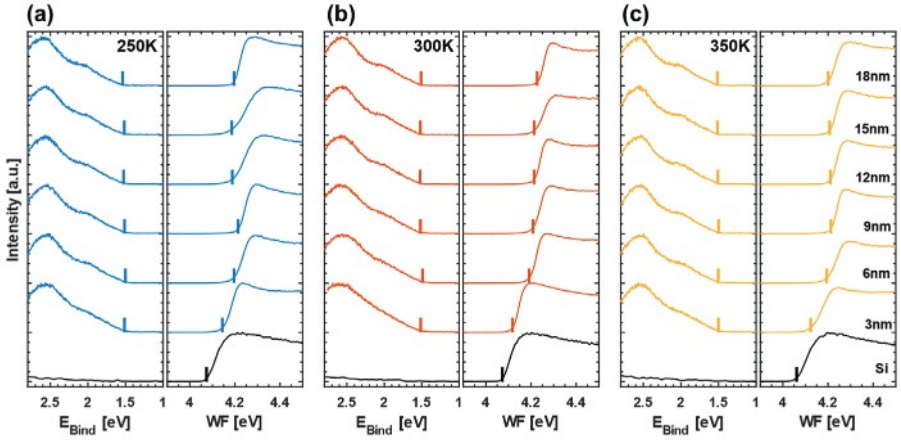

Figure 2. HOMO region (left) and SECO (right) of [6]phenacene on SiO_2 for different substrate temperatures during growth: a) 250 K (blue), b) 300 K (red), and c) 350 K (yellow). For the actual UPS measurements, the samples were allowed to equilibrate to room temperature (≈300 K) and cooled or heated again afterward.

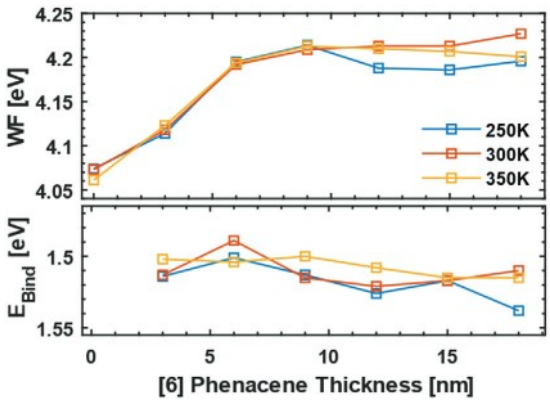

Figure 3. Change of WF and E_{Bind} as a function of [6]phenacene thickness.

However, we find the ionization energy (IE) of [6]phenacene to be thickness dependent. The IE is determined by adding the respective binding energy to the work function (WF), measured from the SECO onset (also indicated by short vertical lines and plotted in Figure 3, top). As can be seen from Figure 3, the value of the IE is mainly governed by the thickness dependence of the WF. It was shown that the precise molecular orientation in ordered molecular assemblies can have a strong impact on the electrostatic surface potential and is influencing the WF and therefore the IE.[10c] In the present case the thickness dependence of the IE can be assigned to the structural change [6]phenacene is undergoing with increasing film thickness (see Figure 1d). This argument is further strengthened when comparing the respective trends for unit cell volume and WF. In both cases the change is most significant for film thicknesses between 3 and 9 nm and comparatively constant for film thicknesses above. The change of IE ranges from 106 meV for the low and room temperature sample to 91 meV for the high temperature sample respectively. Since the substrate Fermi energy (E_F) lies approximately in the middle of the energy gap given by the [6]phenacene HOMO onset ($E_{Bind} \approx 1.5$ eV below E_F) and the estimated LUMO onset position (≈1.6 eV above E_F, obtained by adding the optical band gap of [6]phenacene (≈3.1 eV) to E_F), any effects of gap states on the ELA at the [6]phenacene/SiO_2 interface are unlikely and vacuum level alignment is expected. Since the gap states density is known to reach only a few hundred meV into the gap, there is a too large energy difference to allow for efficient electron transfer between substrate and organic material.[4a,4b]

2.3. UPS Data PFP on [6]Phenacene

Figure 4 shows the thickness dependent UPS data of PFP grown on top of different [6]phenacene bottom layers. On the left-hand side, the PFP HOMO regions are shown. The background signal from [6]phenacene was subtracted for the 3 and 6 nm measurements. The right-hand side shows the WFs obtained from the SECO onset, up to a PFP thickness of 18 nm.

First, we note a temperature dependent initial interface dipole (ID, i.e., difference between WF values) between [6]phenacene and the first 3 nm thick layer of PFP, with values of +100 meV for the low temperature and +30 meV for the higher temperatures. The PFP shows a thickness dependent shift of the WF (Figure 3b, top). However, in comparison to [6]phenacene the trend appears to be more linear with a comparably constant interface dipole when adding an additional material. Furthermore, the observed ID shows a temperature dependence with the total ID between 3 and 18 nm being 137 meV for PFP grown on the low temperature [6]phenacene and 115 and 110 meV for the 300 and 350 K samples respectively. Examining E_{Bind} more closely, we find that, contrary to [6]phenacene, the binding energy does not stay constant, but is decreasing with increasing thickness (**Figure 5**, bottom).

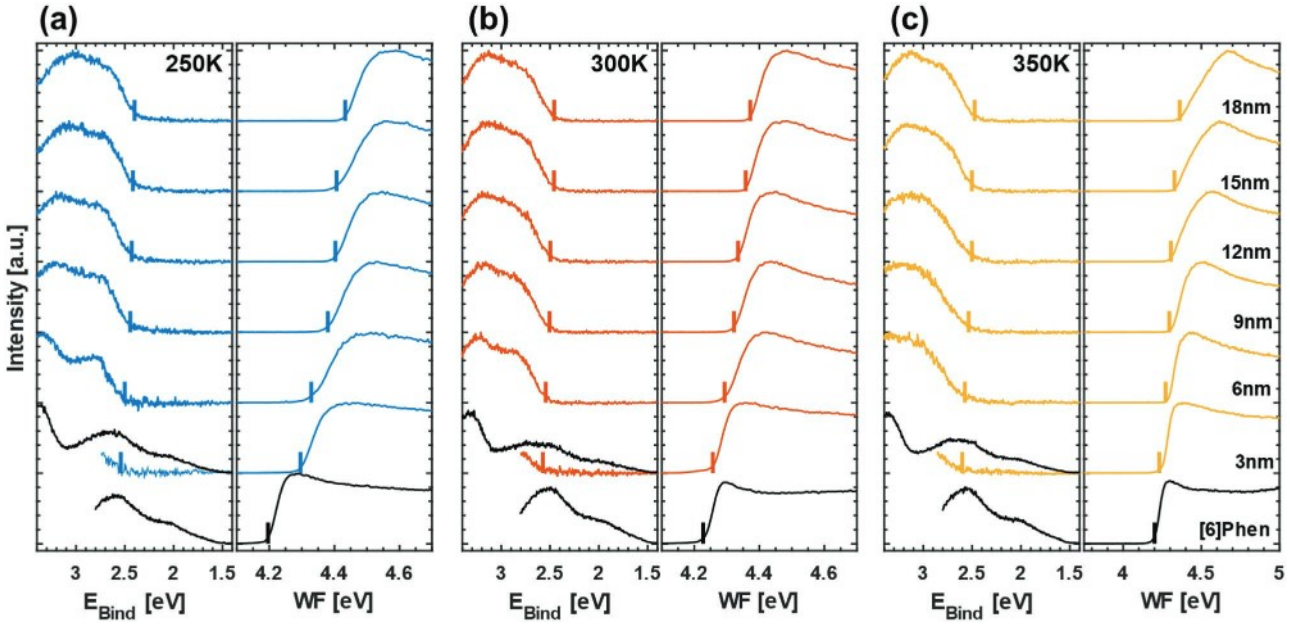

Figure 4. HOMO region (left) and SECO (right) of PFP on [6]phenacene grown at different substrate temperatures: a) 250 K (blue), b) 300 K (red), and c) 350 K (yellow). The [6]phenacene background was fitted and subtracted for the 3 and 6 nm measurements.

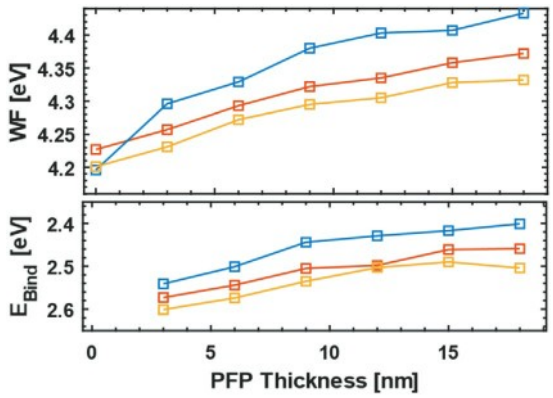

Figure 5. Change of WF and binding energy (E_{Bind}) as a function of PFP thickness.

In addition, this behavior is also temperature dependent with E_{Bind} changing from 2.54 to 2.40 eV ($\Delta = 140$ meV) for low temperature, from 2.57 to 2.46 eV ($\Delta = 110$ meV) for room temperature and from 2.60 to 2.50 eV ($\Delta = 100$ meV) for the high temperature sample. Calculating the IE for PFP we find a rigid shift for E_{Bind} and WF and consequentially, the IE stays constant at an average value of 6.83 ± 0.03 eV for all thicknesses and temperatures. This result is further confirmed by the X-ray data, where we found a thickness independent V_{UC} for PFP and would therefore not expect the IE to change.

The ELA of PFP on [6]phenacene can be rationalized considering structural parameters. As we have seen in Figure 1e, top), D_{coh} of PFP shows a template effect when grown on top of [6] phenacene, with a higher crystal quality for elevated substrate temperatures. As was previously shown, an increase in the density of structural disorder is directly correlated with an increase in the gap state density.

So far, due to experimental restrictions, only a direct measurement of HOMO gap states is possible. The direct detection of gap states reaching out from the LUMO level, which is principally accessible with inverse photoelectron spectroscopy, is still elusive. However, the impact of an altered LUMO gap state density on the ELA can be studied using a conventional UPS setup. This is apparent when adding PFP's band gap of 2.5 eV to the observed E_{Bind}.[15] One finds that the E_F of the substrate lies well within the PFP LUMO distribution, with therefore accessible "empty" electronic states. To establish the thermodynamic equilibrium, electrons are transferred from the SiO_2 into those states in the PFP layer and change the measured WF accordingly. The amount of transferred charges and the absolute value of the ID is now directly dependent on the number of accessible states beneath the substrate E_F (i.e., the density of gap states) which, in turn, can be controlled by changing the crystallinity of the sample.[4e,16] Applying this model to the data presented here, we find qualitative agreement between the density of defects and the observed ID.

3. Conclusion

We presented a detailed investigation of the thickness- and temperature-dependent structural and electronic properties of a [6]phen/PFP heterostructure grown on SiO_2, using in situ X-ray scattering and ultralow background UPS. We find the molecular arrangement of the bottom [6]phenacene layer to be strongly depending on the film thickness, but only slightly impacted by a different growth temperature, additionally, the crystallinity is enhanced for elevated temperatures. A fact that is adopted by the PFP film grown on top via a templating effect. The unit cell parameters of PFP are not changing with increasing thickness and do not show a dependence on the bottom layer's substrate temperature during growth.

Two key findings arise regarding the electronic properties of the heterostructures, which are summarized in **Figure 6**. We find the ionization energy of [6]phenacene to be thickness dependent and correlated with the structural rearrangement the molecules undergo with continuing growth, while no HOMO shift is observed. In contrast, the ELA of PFP depends on the density of gap states that can be attributed to structural imperfections apparent from different sizes of coherently scattering domains. An increased density of gap states due to an increase of structural defects enables a larger number of electrons to transfer from the substrate to unoccupied gap states lying beneath the substrate E_F. Electronically, the bottom [6] phenacene layer thereby simply acts as charge transport layer, however, due to the structural templating effect is ultimately responsible for the magnitude of the level shift of PFP. Our findings show that the spatial distribution of gap states is a key factor affecting the ELA at organic–organic interfaces as well as interfaces between an inert inorganic and an organic material. Moreover, the thickness dependence of the energy shift indicates that an accurate control of the molecular arrangement in thin organic semiconductor films may represent another key factor for controlling the efficiency and functionality of different organic devices.

4. Experimental Section

The X-ray experiments were conducted at beamline I07 of the Diamond Light Source in Didcot, UK using a Pilatus 100K detector and a monochromatic X-ray beam at 13 keV (wavelength 0.95385 Å). Slits directly in front of the detector were used to mimic a point detector where needed. An incidence angle of $\alpha_i = 0.1°$ was chosen for the grazing incidence X-ray diffraction measurements. PFP (99.9% purity) was purchased from Kanto Denka Kogyo Co, [6]phenacene was bought from NARD Co Ltd. (Japan, purity 99.9%). For the UPS measurements, the samples were prepared within the UPS set-up and measurement was conducted without breaking the vacuum ($p < 1 \times 10^{-8}$ mbar). Before installation, the silicon substrates (SiO_2) with a native oxide layer of 2.0 nm were cleaned in an ultrasonic bath with acetone, 2-propanol, and demineralized water successively. Before each sample preparation the substrates were heated to over 700 K overnight to desorb residues. The deposition rates were kept at 2 Å min^{-1}, which was monitored using a water-cooled quartz crystal microbalance during growth. The molecules were evaporated from thermally shielded Knudsen cells. The SiO_2 substrates were mounted on a molybdenum sample holder with options of resistive heating and cooling by liquid nitrogen as required. The substrate temperature was monitored using a thermocouple attached to the sample holder in close proximity to the substrates. UPS was highly surface sensitive with a penetration depth of only a few nanometers, which meant that only the top few molecular layers contributed to the measured data. The substrate WF was similar (variation only 10 meV) for the different samples and measured to be 4.07 eV for the low temperature

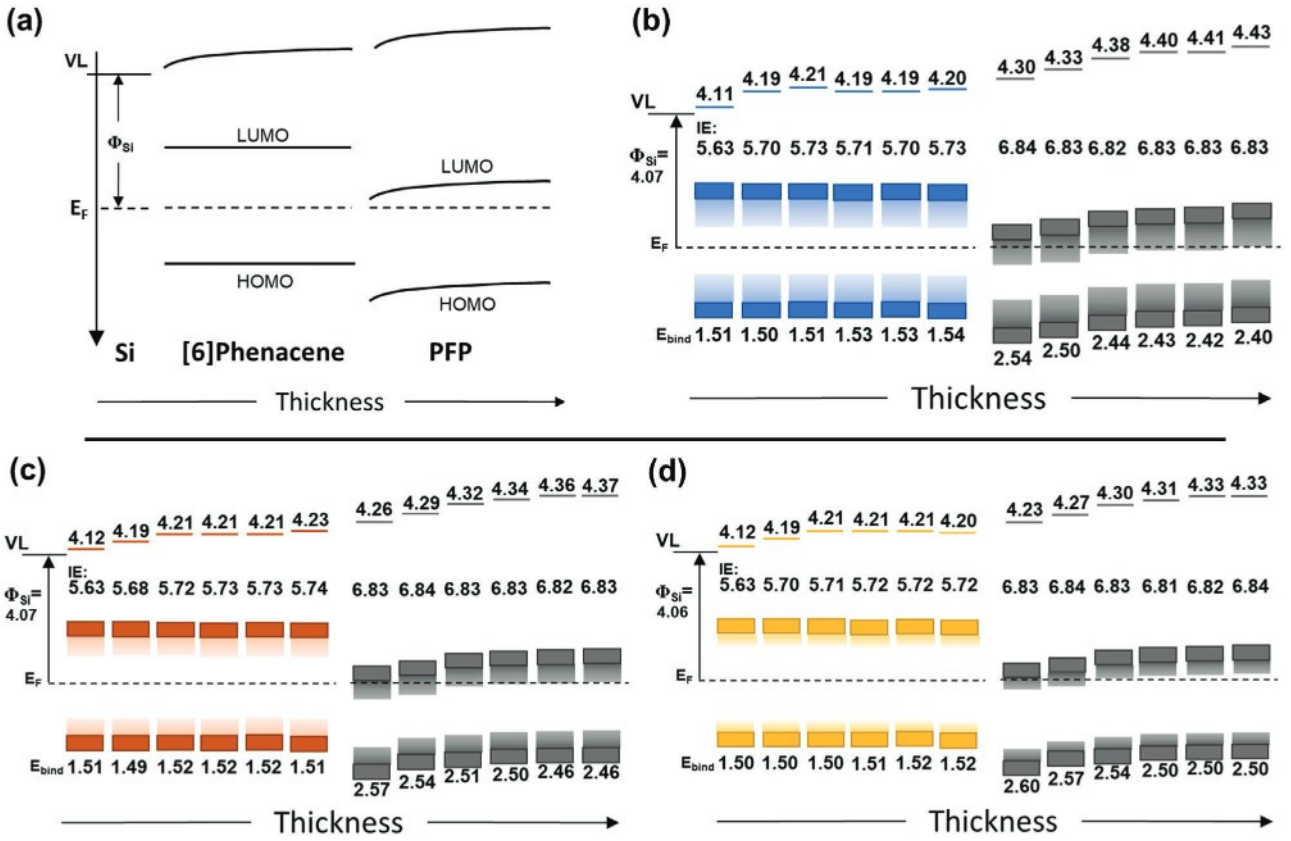

Figure 6. a) Schematic representation of the energy level alignment. b–d) ELA of the three heterostructures with the bottom [6]phenacene layer grown at different substrate temperatures: 250 K (blue), 300 K (brown), and 350 K (yellow). The shading above the HOMO and below the LUMO levels represents the respective gap state density.

and 4.07 and 4.06 eV for the higher temperature samples. Due to experimental restrictions the UPS measurements cannot be conducted in real-time during growth. The data was therefore measured after a new 3 nm thick layer was grown, but without breaking the vacuum. Before each UPS measurement the temperature was equilibrated to room temperature to rule out temperature effects on the UPS data.[14] After the measurement and before starting growth of the next 3 nm layer, the sample was again cooled down or heated up to the desired temperature. The UPS measurements were performed using an ultralow-background, high-sensitivity UPS apparatus with a hemispherical electron analyzer (MBS A-1) and a monochromatic HeI (energy: 21.2 eV) radiation source. All UPS spectra were measured at normal emission with an acceptance angle of ±18°. The He light was incident at 45° with respect to the sample surface. A bias of −5 V was applied to the sample in order to detect the secondary cutoff. The binding energy scale is referred to the Fermi level measured on a metal substrate. Ionization energy values were obtained as $IE = E_{HOMO} + \Phi = E_{HOMO} + h\nu - E_{cutoff}$, where Φ is the work function of the sample, defined by the energy separation of the vacuum level from the Fermi level. E_{HOMO} is the HOMO edge position and E_{cutoff} is the cut-off position.

Supporting Information

Supporting Information is available from the Wiley Online Library or from the author.

Acknowledgements

The Diamond Light Source (DLS) is gratefully acknowledged for providing the authors with beamtime under proposal number 18570 and thank the staff from I07 for their support. This work was supported by the German Research Foundation (DFG) under project HI 1927/1-1. J.H. thanks the Japan Society for the Promotion of Science (JSPS) for funding during the Summer Program in Japan.

Open access funding enabled and organized by Projekt DEAL.

Conflict of Interest

The authors declare no conflict of interest.

Data Availability Statement

The data that support the findings of this study are available from the corresponding author upon reasonable request.

Keywords

energy-level alignment, gap states, organic semiconductors, structural defects

Received: July 30, 2021
Revised: October 18, 2021
Published online: December 17, 2021

[1] a) D. Kim, V. Coropceanu, J.-L. Brédas, *J. Am. Chem. Soc.* **2011**, *133*, 17895; b) N. Koch, *J. Phys.: Condens. Matter* **2008**, *20*, 184008;